Geosciences Journal
Vol. 20, No. 1, p. 101 − 115, February 2016
DOI 10.1007/s12303-015-0020-7

Modification of a digital elevation model (DEM) in a flat topographic area with respect to manmade features

Wael Kanoua* — *Department of Petroleum Engineering, Chemical and Petroleum Engineering Faculty, AL Baath University, Homs, Syria*
Department of Hydrogeology, TU Bergakademie Freiberg, Gustav-Zeuner Str. 12, 09599 Freiberg, Germany
Broder J. Merkel — *Department of Hydrogeology, TU Bergakademie Freiberg, Gustav-Zeuner Str. 12, 09599 Freiberg, Germany*

ABSTRACT: This study compares two Digital Elevation Models (DEMs) that are available free of charge: (1) the Consultative Group for International Agriculture Research Consortium for Spatial Information SRTM C-band CGIAR-CSI v4.1 (SRTM): 3 arc sec (approximately 92 m at the equator; originally 1 arc sec but only distributed with 3 arc sec) and (2) the Advanced Spaceborne Thermal Emission and Reflection Radiometer-Global Digital Elevation Model ASTER GDEM v2 (ASTER2): 1 arc sec (approximately 31 m at the equator). Additionally, the DEM was modified according to known topographic features in the study area. The first step was investigating whether there is a spatial shift between the different DEMs by using a very high resolution (VHR) satellite GeoEye image. Beside visual comparisons, statistical methods were applied to compare the elevation models. Reference data used in this study are the Ground Control Points (GCPs) collected in a previous investigation in the same study area. SRTM proved to be the better of two available free elevation models (SRTM and ASTER2). This conclusion is based on an assessment of the different investigated aspects such as morphologic details, reliability, completeness, and accuracy. The ability to modify the SRTM model with 92 m horizontal resolution from the Shuttle Radar Topography Mission is here discussed. The study area is located in Titas Upazila, Comilla district, Bangladesh and comprises manmade topographic features (e.g., road embankments and mounds that houses are built on above the monsoon flooding level), which are not or not completely represented in the DEM due to their small spatial extent. To represent these topographic features, the DEM was refined by dividing each pixel into 0.5 m pixel spacings. The elevated areas (roads and villages) were digitized using GeoEye satellite imagery and Google Earth. The pixels located in the elevated areas were given the proper elevation and rejoined to the original DEM raster. The effect of trees can be excluded because of their scarcity in the studied area, and because their existence is limited just to both sides of the artificially elevated streets and areas where people live. Furthermore, the bias in the SRTM model is eliminated by two steps: (1) the mean (value) of the differences between the GCPs and the corresponding points of the SRTM is subtracted from SRTM points, and then the root mean square error (RMSE) is diminished to 0.67 m; (2) the same mean (value) of the differences is subtracted from the whole SRTM model. The finally modified DEM represents the real terrain surface with the most important details of the study area. This modified elevation model may be used in studies to model groundwater flow driven by topography.

Key words: digital elevation model (DEM), ASTER GDEM v2 (ASTER2), SRTM C-band CGIAR-CSI v4.1 (SRTM), Bangladesh, GeoEye

*Corresponding author: wael_kanoua@yahoo.com

1. INTRODUCTION

Elevation models are essential tools in many applications (Small, 1998; Guo-an et al., 2001; Konstantinos and Antonis, 2004; Hirt et al., 2010). Examples of these applications are topographic cartography, flood simulation and the detection of flood-prone areas, gravity field modeling, pedology, economics, agriculture, groundwater modeling, modeling distributed hydrological processes, mass movement investigations, spatial and temporal change detection (Hirt et al., 2010; Sertel 2010; Saldana et al., 2012; Pilesjö and Hasan 2014), ecology (Sunahara et al., 2003), forestry (Simard et al., 2006), the construction and maintenance of different facilities (Konstantinos and Antonis, 2004), oil and gas exploration (Arefi and Reinartz, 2011), mitigating the effects of natural disasters like landslides and land subsidence (Chorowicz et al., 1998; Singhroy et al., 1998; Small, 1998; Ahmad, 2009), and the detection and mapping of ancient settlement mounds in the field of archeology (Menze et al., 2006; Casana and Cothren, 2008).

Elevation models are of vital importance in earth science, especially for hydrologists and hydrogeologists, because the topographic surface affects the processes occurring on the ground surface and in the subsurface, for example, surface flow directions, surface runoff, stagnant zones of surface water, and subsurface flow driven by topography. Moore et al. (1991) presented a detailed review of the main hydrological, hydrogeological, and morphological applications of DEMs. DEMs are used to extract drainage networks (after hydrologic corrections) and surface flow areas that contribute to sediment loads (Lane et al., 1994). Furthermore, accurate topography can be used to develop more physically realistic structures for hydrologic and water quality models that directly account for the impact of topography. Luijendijk et al. (2010) showed the effect of topography-driven groundwater flow on the distribution of subsurface temperature. Contaminant distribution in groundwater is also affected by topography because the groundwater level more or less follows the topography of the area, which in turn alters the flow paths in the subsurface.

Taking everything into account, either ignoring the effect of topography on the flow field or giving wrong representation of

the topography in hydrogeological modeling is a crucial error. It may result in a biased outcome of the interpretation of modeling results that concern the movement of contaminants and their distribution in the subsurface. This effect of topography is more pronounced in humid regions where topography is the most important driving force in groundwater flow (Creed and Sass, 2011). Therefore, care should be taken if it is decided to use a DEM as the only alternative in areas where no detailed topographic maps are available. In other words, a DEM should be as accurate as possible and comprise almost the entire topographic features of the study area.

Which of the freely available DEMs is the most appropriate for an application is often unclear; thus, in this study it was decided to perform a qualitative evaluation of both DEMs (SRTM and ASTER2) by considering morphologic details, completeness, and accuracy. The aforementioned manmade topographic features (e.g., road embankments and mounds on which houses are built above the monsoon flood level) are missing due to the coarse resolution and the small size of the features. These missing features are presented in the final DEM, which has a resolution of 0.5 m. Sections 2 and 3 present an overview of the different freely available DEMs and their accuracy. The study site and data description are presented in Section 4, followed by the methodology in Section 5, the results and discussion in Section 6, and an attempt to modify the SRTM elevation model in Section 7. The conclusions follow in Section 8.

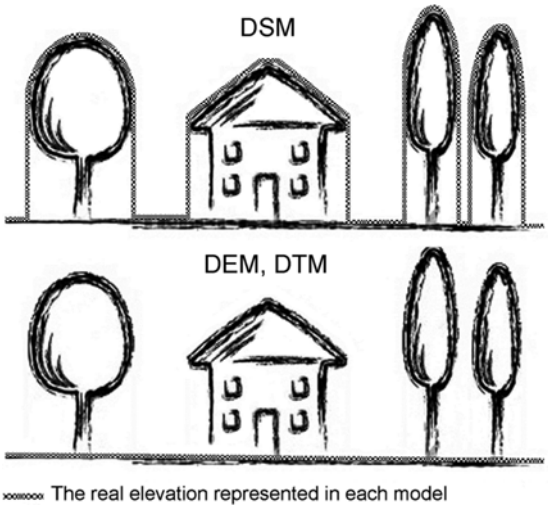

Fig. 1. Schematic representation of Digital Surface Model, Digital Elevation Model and Digital Terrain Model.

2. DIGITAL ELEVATION MODELS (DEMs)

DEMs are digital representations of elevation values at different points above some datum in a special geographic area (Moore et al., 1991). Data from field surveys, Global Positioning System (GPS) surveys, photogrammetry, satellite remote sensing, airborne laser altimetry, and digitizing the already existing topographic maps are considered the main sources used in creating DEMs (Konstantinos and Antonis, 2004). However, in many cases elevations are interpolated from the digitized contour lines of pre-existing maps. Typically, the contour lines on these maps were created from stereo aerial photographs. More recently, the creation of DEMs from images and then deriving contours from the DEM has become a commonly performed task (Bekithemba et al., 2001).

It is worth mentioning here that different terms such as Digital Surface Model (DSM), Digital Elevation Model (DEM), and Digital Terrain Model (DTM) are used in the literature, which may cause confusion to some readers because the different terms are sometimes used interchangeably. However, there is inherently a big difference between them, with the exception of areas where no artificial or natural ground cover exists (e.g., deserts). The above definition is applicable to these three models (DSM, DEM, & DTM); nevertheless, the represented elevation values are not identical for the same pixel in all models. Looking at Figure 1, the main difference can easily be grasped. DSM is the main and first elevation product of photogrammetry, comprising the elevations of the bare soil surface and the tops of all other features (vegetation, buildings etc.) existing on the sensed topographic surface. On the other hand, the DEM and DTM are the filtered results of a DSM that eliminate artificial (buildings) and natural (vegetation, snow) elevations not belonging to the bare soil (Jacobsen, 2003; Braun and Fotopoulos, 2007). In ice sheet areas (Antarctic and Greenland), a DEM which describes the top of ice sheets is referred to as an "Ice Surface Model," and one which describes the base of the ice sheets is referred to as a "Bedrock Model". The difference between DEM and DTM is that, beside the relief, DTM also represents its description as slope, aspect, contour lines, break lines, and peaks (Martinoni and Bernhard, 1998; Podobnikar et al., 2000). In general, DEM is used as a general term without specifying whether it is DSM or DTM. This definition was unclear a few years ago, but today it is the generally accepted definition.

There are different resources available for acquiring DEMs at no charge including the following examples: the GTOPO30: 30 arc sec global dataset (~1 km pixel size); the Shuttle Radar Topography Mission C-band SRTM: 3 arc sec (1 arc sec for USA, Canada and some special areas); the X-band SRTM: 1 arc sec; the Thermal Emission and Reflection Radiometer ASTER GDEM: 1 arc sec, and existing digitized topographic maps. A complete compilation of the latest versions of the currently freely available global DEMs is listed in Rexer and Hirt (2014) in chronological order with their respective resolutions. The satellite-based elevation datasets are DSMs because they almost represent the heights of the first reflective surface (surface features) in comparison to the elevation models created from already existing topographic maps (Jacobsen, 2008; Sefercik and Alkan, 2009; Hirt et al., 2010).

3. ACCURACY OF FREELY AVAILABLE DEMs

Three types of errors may be defined for a DEM: planimetric errors (in x and y coordinates), vertical errors (elevation; z coordinates), and errors related to the pixel size. The first two kinds of error are due to an erroneous elevation at a correct location or to a correct elevation at an erroneous location, or to both of these (Nikolakopoulos et al., 2006). The relative and absolute error also has to be distinguished. It is not possible for SRTM and ASTER to assess individual location error, and only the shift values for the whole height models are assessable. The vertical and horizontal accuracies are not equal in all the available models and need to be checked. The accuracies of some elevation models have previously been checked over certain areas and found to increase in the following ascending order: C-band SRTM 30 → Google Earth → Digitized Topographical map (Isioye and Jobin, 2012).

The (3D) positional accuracy (in x and y coordinates and z elevation) of the elevation model has been assessed by comparing the planimetric coordinates and elevation of the sample points on the images against the planimetric coordinates and elevation of the same points derived from any source more accurate than the images (Congalton and Green, 2008). The accuracy is reported by means of the RMSE or by applying the standards developed by the Specifications and Standards Committee of the American Society for Photogrammetry and Remote Sensing (ASPRS), whereby the determination of accuracy depends on calculating the RMSE values from check points and then proceeding further in the accuracy of the result by means of scale maps. Furthermore, the National Standard for Spatial Data Accuracy (NSSDA) also reports the accuracy of digital geospatial data at the 95% confidence level as a function of RMSE values in x, y, and z at ground scale (ASPRS Map Accuracy Working Group, 2014).

The best accuracy for an elevation model can be obtained by using a total station, which is an electronic/optical surveying instrument for measuring horizontal and vertical angles and distances (Kavanagh and Bird, 2000); however, using a total station is costly and time consuming. Depending upon the terrain's properties, airborne laser scanning (ALS) also derives height and horizontal accuracies in the range of 0.1~0.5 m and 0.3~1.5 m, respectively (Turton and Jonas, 2003); however, the cost of ALS is relatively high for some applications. Therefore, for this study SRTM and ASTER2 were used. GTOPO30 (30 arc sec) was not suitable because of the way off to coarse resolution and the X-band SRTM is not available for this area of interest. Many studies have been conducted to estimate and compare the accuracy of ASTER GDEM and C-band SRTM elevation models. The following is a short review of these.

ASTER GDEM, with a spatial resolution of 1 arc sec (approximately 31 m at the equator), is the highest DEM resolution among the available free DEMs (with the exception of X-band SRTM with the same resolution of 1 arc sec, but with 40% earth coverage); it is generated from original 15 m resolution optical digital stereo ASTER images. Horizontal and vertical accuracies of ASTER GDEM are estimated to be 30 m and 20 m RMSE respectively at the preproduction level at the 95% confidence level (Arefi and Reinartz, 2011). Hirano et al. (2003) evaluated the vertical accuracy of ASTER DEM at four test sites, and their results revealed a RMSE of elevation of between 7 and 15 m. Hirt et al. (2010) also found the vertical accuracies of national GEODATA DEM-9S v3, SRTM v4.1, and ASTER GDEM v1 over Australia using GCPs to be RMSE 9 m, 6 m, and 15 m, respectively. In a following study, Rexer and Hirt (2014) compared the latest release of ASTER GDEM v2, SRTM3 USGS v2.1 with SRTM C-band CGIAR-CSI v4.1 and evaluated their accuracy against the ground truth dataset for Australia. They reported elevation accuracies to be RMSE 8.5 m, 6 m, and 4.5 m for ASTER GDEM v2, SRTM3 USGS v2.1, and SRTM CGIAR-CSI v4.1, respectively. Using validation points from Global Navigation Satellite Systems (GNSS), Athmania and Achour (2014) assessed the vertical accuracy of the ASTER GDEM v2, CGIAR-CSI SRTM v4.1, and GMTED2010 at two test sites in Tunisia and Algeria. The RMSE of CGIAR-CSI SRTM v4.1 model (3.6 m) indicated a higher vertical accuracy than ASTER GDEM v2 (5.3 m) and GMTED2010 (4.5 m) for both sites. Reuter et al. (2009) used different methods to evaluate the horizontal and vertical accuracy of ASTER GDEM, and found the RMSE for GDEM to be 18 m and 29 m, respectively, and 10–15 m for SRTM. By using a reference DEM from a topographic map (1:5,000 scale) to analyse the accuracy of ASTER DEM over Istanbul, Sertel (2010) concluded that ASTER GDEM showed the main topographic features of the studied area. However, the absolute error in elevation was estimated to be 20 m in most of the studied region, and higher than 20 m in some parts.

C-band SRTM (approximately 92 m at the equator) is generated from radar images (λ = 5.6 cm) from NASA's space shuttle. C-band SRTM DEMs are available for 80% of the globe. Vertical and horizontal accuracies of C-band SRTM DEM 1 arc sec are estimated to be 20 m and 16 m (linear error at 90% confidence), which can be described as a RMSE of 12 m and 10 m, respectively (Smith and Sandwell, 2003; Nikolakopoulos et al., 2006). In Istanbul (6000 km^2 test field), Yastikli et al. (2006) assessed the accuracy of GTOPO30 and DEMs from SRTM X- and C-bands in comparison with the reference DEM from topographic maps (1:25000 scale) and GCPs; they found similar vertical RMSE values for both X- and C-bands using a reference DEM from a topographic map. However, the RMSE differed between the two bands (5.6 m and 9.6 m for X- and C-bands, respectively) when using GCPs. Rodriguez et al. (2006) concluded in a global validation study that for C-band SRTM DEM the absolute elevation error exceeded the mission's goal (16 m) by a factor of two. Jarvis et al. (2004) evaluated the absolute difference between C-band SRTM DEM and a DEM derived from a

1:50,000 contour map in Honduras. They concluded that C-band SRTM DEM has a 8 m RMSE compared to 20 m for the topographic DEM, which means that the C-band SRTM DEM is more accurate than the 1:50,000 scale cartographically derived DEM for Honduras.

4. DATA

4.1. Study Area

The study area is located in Titas Upazila in the Meghna flood plain, south east of Bangladesh. It is east of the Meghna River, 50 km south-east of Dhaka (capital city of Bangladesh) in the Comilla District of the Chittagong division, Bangladesh. Titas is bounded by Homna to the north, Daudkandi to the south, Muradnagar to the east, and Meghna to the west. There is a natural border to the north provided by the Titas River, to the west by the Meghna River, and to the south and east by the Gumti River (Fig. 2). Geographically, the location of Titas is 90°40′E, 23°31′N for its southwestern corner and 90°52′E, 23°52′N for its northeastern corner.

Elevations in Bangladesh reach 105 m above sea level in the northern parts; however, the elevation is much lower for the rest of Bangladesh and in many places is less than 10 m. The terrain in the coastal areas is generally at sea level, either very close to it or in some places below sea level. The aforementioned low elevation topography and the triple river system plus the dense river network in Bangladesh make most parts of the country prone to flooding.

The topography of the study area (Titas) is more or less flat (0–25 m above sea level), and comprises irregularly shaped artificial "islands," on which houses are built above the monsoon flooding level, surrounded by low lying areas which are mostly cultivated lands and water bodies (Kanoua and Merkel, 2015). These topographical features are normal and also found in other parts of Bangladesh (Harvey et al., 2006; Khan et al., 2011). These elevated areas are constructed by excavating soil to build dams and small plateaus to protect the houses and roads against flooding. As a consequence, there are many excavation pits in the region of interest.

4.2. Data Preparation

Table 1 summarizes the data used in this study. SRTM C-band CGIAR-CSI v4.1: 3 arc sec was downloaded in Geotiff format from Consultative Group for International Agriculture Research Consortium for Spatial Information (CGIAR-CSI) (http://srtm.csi.cgiar.org). ASTER GDEM v2: 1 arc sec was downloaded from the Earth Remote Sensing Data Analysis Center (ERSDAC) (http://www.jspacesystems.or.jp/library/archives/ersdac/eng/index.E.html). ASTER GDEM v2 is provided with a Geotiff file that records numbers (stack numbers) representing the number of individual scene DEMs that were stacked to create the final averaged DEM elevation value (see Section 6.1). Both datasets were provided in a geographic latitude/longitude coordinates with the WGS84 (World Geodetic System, 1984) horizontal datum and mean sea level as vertical datum. The GCPs used in this study were taken from a previous study of the same area of interest by Planer-Friedrich et al. (2012); these GCPs were collected using total station and the data were provided in a geographic latitude/longitude coordinates with the WGS84 horizontal datum and mean sea level as vertical datum. The GCPs have a planimetric accuracy of 10–15 cm (RMSE) and a vertical accuracy

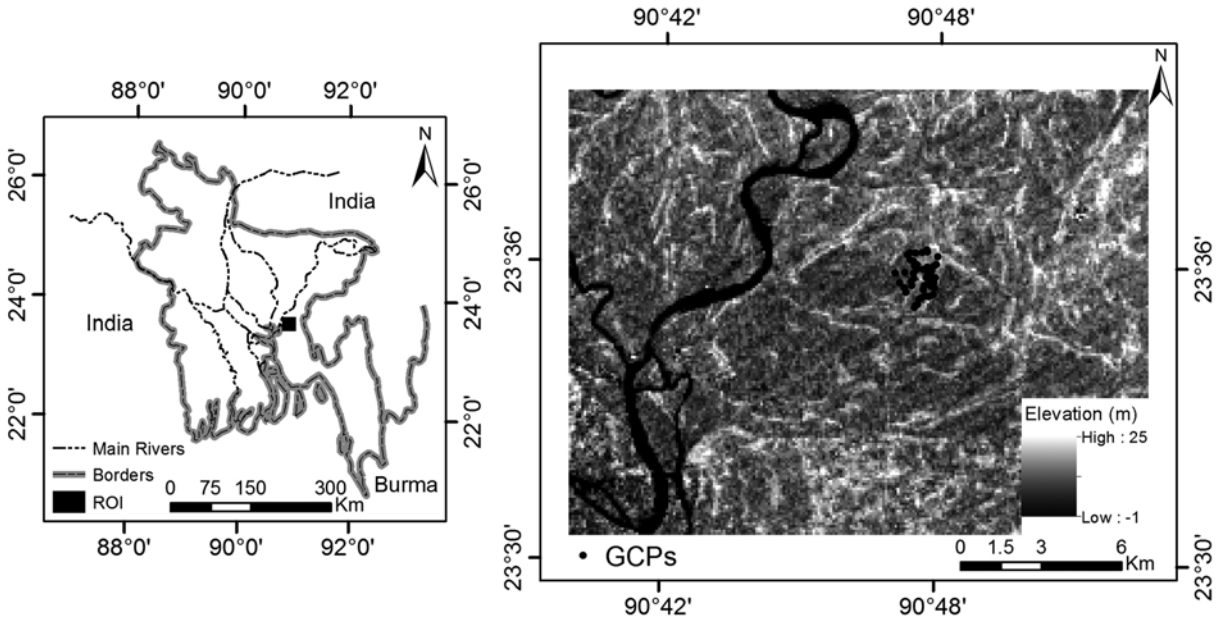

Fig. 2. Map of Bangladesh (left) and the study area (right) in Titas Upazila with the black dots representing the GCPs.

Table 1. Data used in this study comprises two elevation models SRTM C-band CGIAR-CSI v4.1 and ASTER GDEM v2 and 57 Ground Control Points (GCPs) with their basic features

	SRTM C-band CGIAR-CSI v4.1	ASTER GDEM v2	57 GCPs (reference data)
Instrument	Space Shuttle Radar C/X-band SAR	ASTER (optical)	Total Station
Coverage	+60 N to –56 S latitude	+83 N to –83 S latitude	–
Coordinate System	GCS	GCS	GCS
Horizontal Datum	WGS84	WGS84	WGS84
Vertical Datum	Mean Sea Level	Mean Sea Level	Mean Sea Level
Resolution m/arc sec	92 m/(3 arc sec)	30 m/(1 arc sec)	–
Elevation Accuracy	<16 m (at 90% confidence)	<17 m (at 95% confidence)	0–9.8 cm (at 95% confidence)
Format	Raster (TIFF)	Raster (TIFF)	Table (CSV)

WGS84: World Geodetic System 1984.

of 0–5 cm (RMSE). The corresponding accuracies at the 95% confidence level according to the NSSDA are 24.5–36.7 cm and 0–9.8 cm, respectively. All the datasets were projected to UTM WGS84. In the following SRTM C-band CGIAR-CSI v4.1 and ASTER GDEM v2 will be referred to as SRTM and ASTER2, respectively.

5. METHODOLOGY

In this paper, the two DEMs are compared: ASTER2 and SRTM. The ASTER Quality Assessment (QA) File (num-file) was first investigated to see the distribution of the number of stacks in the study area. Spatial positioning (i.e., latitude and longitude) shift in elevation models is a well-known problem, which has to be checked and corrected as the first step before any kind of elevation comparison is performed with reference data. Normally, horizontal shifts are estimated by the adjustment of the DEMs against a reference height model (Jacobsen and Passini, 2010). However, such a reference height model is not available for the study area of this research paper, so the shift of the DEM models was checked with the help of a VHR GeoEye satellite image, which was provided from a grant by GeoEye Foundation Employee Advisory Committee (FEAC). The shift is assessed by comparison of the centroids of extracted features from the ASTER2 and SRTM datasets with the same features from the GeoEye image. Visual analysis was undertaken as a qualitative method to compare the DEMs. For visual comparison, two approaches were used: shaded relief and topographic cross sections are the easiest and most-effective ways of comparing different DEMs visually. Shaded relief is by definition a way of showing changes in elevation in a raster image by using light and shadows on terrain from a given angle and altitude of the sun, which helps the map users to perceive the forms of the earth surface relief. Moreover, topographic cross sections through the two different DEMs are a useful visual technique. In some cases, cross sections can help to detect any planimetric shift in the data and deliver an idea of the different inclinations of the compared surfaces. Statistical analyses, in contrast to visual comparison, are used to evaluate the DEMs quantitatively. The reference data used here are the 57 GCPs. The Spearman correlation test (two-tailed) was used, and the elevation difference between the GCPs and the corresponding points from the other two DEMs was analysed. In addition, RMSE was used to quantify the vertical accuracy of DEMs.

6. RESULTS AND DISCUSSION

6.1. ASTER Quality Assessment (QA) File

Due to the fact that the first version of ASTER GDEM was not perfect (poor elevation data), stacking and filtering was used to improve the quality and reduce bad elevation data (Urai et al., 2012). Stacking has been proposed as the simplest and most effective method to reduce bad elevation data in the ASTER GDEM. It is done by adding new observation data and regenerating the elevation model. The accuracy of ASTER GDEM depends on the number of individual scene DEMs that were stacked to create the final averaged DEM elevation value; in other words, its accuracy depends on the number of stacks/point. The ASTER Global DEM Validation Summary Report 2011 gave a rough global overview of the number of used stacks (number of used ASTER images). The number of stacks for any object point is inferred from the num-file (quality assessment [QA] file) distributed and downloaded together with the ASTER GDEM. It can vary strongly within the 1° × 1° individual ASTER GDEM tile.

The number of stacks in the study area reaches 19 with a mean value of 14 and a standard deviation SD = 1 (Fig. 3). This means that a maximum up to eight stereo models were used to determine the object points. The distribution of the number of stacks is shown in Figure 4. The lowest number of stacks (4–6) is available in water areas, which means that the smaller the stack number, the worse the data quality. Moreover, Figure 4 (right) shows strips oriented south-north in the stacking number map. These strips are attributed to an inadequate number of observations, which might cause "step anomalies" as artifacts in the corresponding ASTER elevation model (Tachikawa, 2011). However, in looking at the corresponding ASTER2 (Fig. 4, left), the step anomalies have

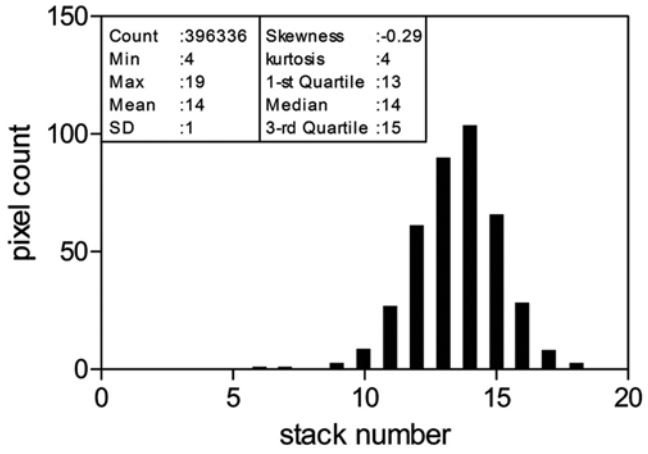

Fig. 3. Histogram and statistics of the num-file of ASTER2 model for the study area. 'Stack number' on x axis represents the number of individual scene DEMs that were stacked to create the final averaged DEM elevation values.

no effect due to the increasing number of scenes used to produce the final ASTER elevation model.

The relationship between the mean and RMSE and the stacking number was investigated by Tachikawa (2011). They found that big errors are associated with fewer than ten scenes, and especially fewer than three scenes. The reduction in the error is significant between one and ten scenes, but there is little improvement over about 15 scenes. Moreover, Jacobsen and Passini (2010) studied the relation between RMSE and the number of stacks in different areas. They reported the general relationship between the average of stacks/point and the RMSE for ASTER GDEM v1 as:

$$\text{RMSE} = 12.43\ \text{m} - 0.35\ \text{m} * \text{number of stacks/point}. \quad (1)$$

If the same relation holds for ASTER2, Equation (1) enables the accuracy of ASTER2 to be quantitatively estimated. Applying Equation (1) of this study case (average of stacks/point = 14) results in the RMSE of 7.53 m.

6.2. Spatial Shift

Many researchers have reported this problem for different DEMs (ASTER Global DEM Validation Summary Report, 2009; Guth, 2010). Frey and Paul (2012) reported a 55 m spatial shift in the SRTM DEM in a south-west direction, and mentioned that this shift depends on the respective download source. Nikolakopoulos et al. (2006) compared SRTM and GDEM for two regions in Greece and found a spatial shift in SRTM data of 200 m and 400 m in eastern and northern directions, respectively. Here, it is worth mentioning that the geolocation of SRTM is rather better, which means that these shift values of 200 m/400 m are definitely caused when SRTM-derived DEM was reprojected from UTM WGS84 to the Hellenic Geodetic Reference System 87 (HGRS87). Using elevation matching, Gonçalves and Morgado (2008) were able to detect the horizontal shift of SRTM data, and they used this method to correct different maps with an elevation component regarding the spatial shift. Rexer and Hirt (2014)

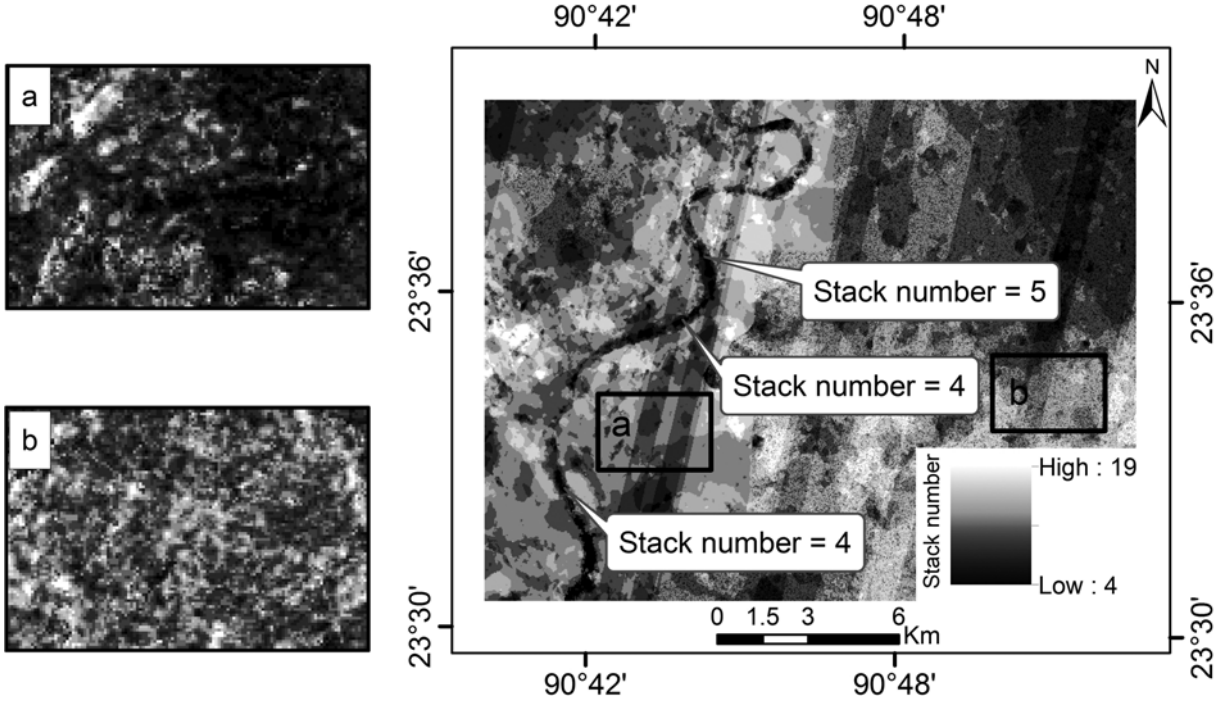

Fig. 4. ASTER2 stacking number map showing numbers of ASTER DEMs contributing to the ASTER2 in the study area (right) and ASTER2 elevation of some spots (a and b) from the same area (left).

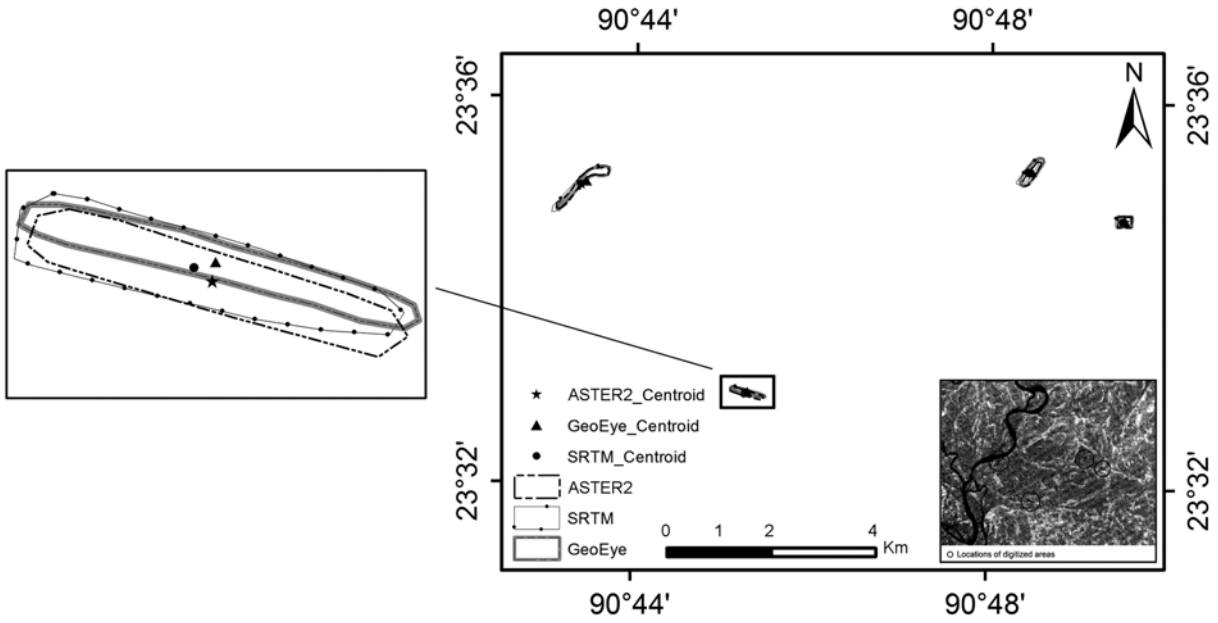

Fig. 5. Four Digitized areas from GeoEye, SRTM, and ASTER2 to investigate the spatial shift in the different models. Centroids of the elevated features (left) are represented as triangle for GeoEye, star for ASTER2, and circle for SRTM.

showed a mean relative shift for ASTER2 compared with SRTM of –0.007 and –0.042 arc sec in a north-south direction and –0.100 and –0.136 arc sec in an east-west direction using 529 1 × 1 degree tiles and 138 2 × 2 degree tiles over Australia, respectively.

The shift of the DEM models was checked with the help of a VHR GeoEye satellite image. GeoEye satellite imagery is considered to be the most detailed satellite imagery so far available to the public. It locates an object within just 4 meters of its physical properties. The satellite image was provided with 0.41 m and 1.65 m resolutions in panchromatic and multispectral (Blue, Green, Red, and Near Infra-Red) bands, respectively. The final multispectral 0.5 m image was created using the pan-sharpening function in the Earth Resources Data Analysis System ERDAS IMAGINE (Leica Geosystems, Atlanta, GA, USA) software. Four features (elevated areas) were digitized (Fig. 5), which were completely clear on both SRTM and ASTER2, as well as on the GeoEye image. These elevated areas have a stack number of 14–16 for ASTER2. The spatial comparison was done between the coordinates of the centroids of the same feature from the three datasets, and it revealed a fairly consistent shift in latitude and longitude for each elevation model relative to the GeoEye. The calculations showed a spatial shift as an average value of the shifts of the four centroids of about 53 m in x direction and 11 m in y direction for SRTM, and 26 m in x direction and 24 m in y direction for ASTER2. The 4 m spatial accuracy of the GeoEye satellite image makes its use as reference data for spatial shift plausible. This spatial shift in both directions was corrected in the geographic information system ArcGIS Desktop 9.3 (Environmental Systems Research Institute (ESRI), Redlands, CA, USA) (Shift-Data Management) before performing any further analysis.

6.3. Visual Comparison

Figure 6 represents shaded relief maps of the different DEMs created in ArcGIS Desktop 9.3 using the Hillshade tool. A river channel on the left side of this area of interest is clearly represented in SRTM, but not in ASTER2. Such artifacts in DEMs are considered to be the worst visual anomalies of the ASTER elevation models. In spite of improved water masking in ASTER2, artifacts are still found over some water stream channels and surface water areas in ASTER2 (Tachikawa, 2011). This is due to the absence of an inland water body mask for some areas in the algorithm: the elevation values of some water body regions are not set to a single "flattened" elevation value (Stevens et al., 2004; ASTER Global DEM Validation Summary Report, 2009; Arefi and Reinartz, 2011). These water body artifacts can be corrected by using SRTM data (Guth, 2010). ASTER2 also involves artifacts and anomalies that are responsible for big vertical errors, especially on a local scale (Arefi and Reinartz, 2011).

Moreover, topographic cross sections of the DEMs are a useful visual technique for comparing different DEMs. Figure 7 superimposes two topographic cross sections through the two DEMs in the x and y directions, as shown in Figure 6. The continuous and dashed curves represent the ASTER2 and SRTM, respectively. The SRTM model was first resampled to 30 m spatial resolution (using the Nearest Neighbor (a), Bilinear (b), and Cubic (c) techniques) to match the ASTER2. Small-scale topographic fluctuations were removed

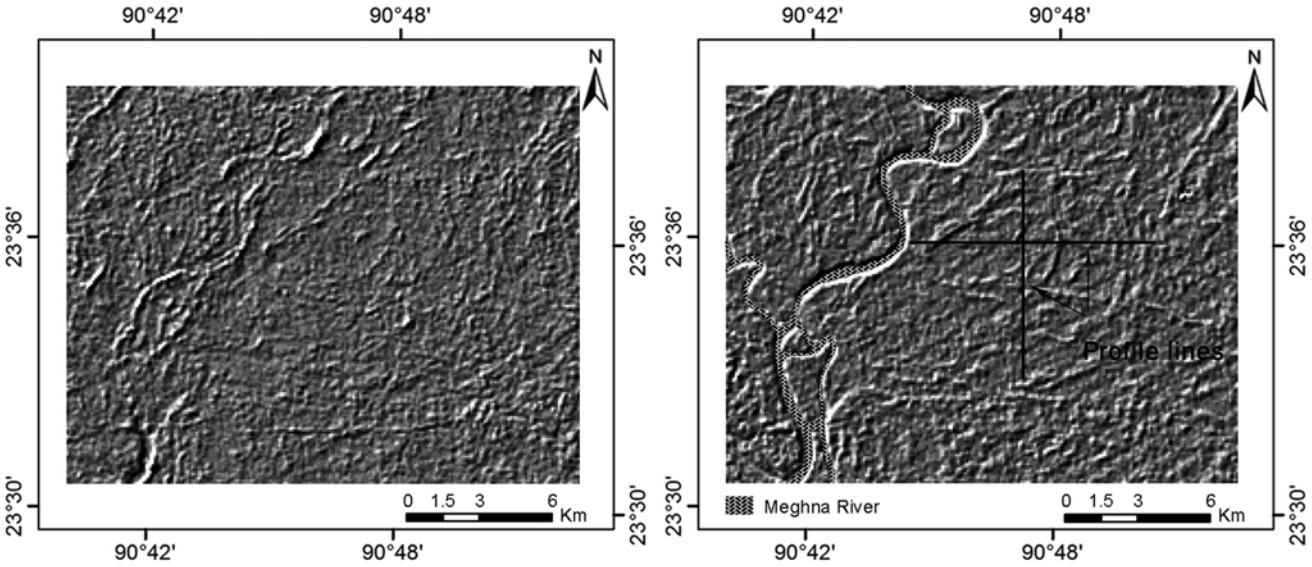

Fig. 6. Shaded relief maps of the ASTER2 (left) and SRTM (right) in Titas Upazila.

by simple moving averages. In a simple moving average, the sum of the data points over a given period is divided by the number of periods; in other words, data are averaged successively within each defined period. Simple moving averages with different periods (2, 5, 10, and 15) were tested and the result for the 10-period moving average is presented in Figure 7. The two profiles do not show clear relations between the two models using the three resampling techniques; they only show that the topographic profile of ASTER2 is nearly as high as that of the SRTM model along both the x and y cross sections. The elevation means of ASTER2 and SRTM are 8.7 and 6.8 with SD of 2.3 and 2, respectively. Moreover, the linear trends through the profiles of the two datasets are shown as dashed and continuous straight lines on the same charts. Looking at the trend lines of the longitudinal and latitudinal profiles of the three resampling cases, one can notice the difference in slope in the latitudinal direction. This has of course a high impact in hydrological applications. SRTM represents a steeper surface towards the west than ASTER2; however, one can see an evident difference towards the south. SRTM shows an inclination towards the south, while the inclination in ASTER2 is to the north. The investigation found that the mean stack number of all pixels along both profiles was 14 and 13 with a SD of 1 for the latitudinal and longitudinal profiles, respectively. The opposite inclination in the case of ASTER2 may be the results of its sensitivity to the sparse vegetation cover (presented in the southern part of the study area in comparison to the southern and northern parts), which means it probably offers a so-called "Digital Canopy Model." On the other hand, the reflectance level of SRTM C-band is approximately one third below the canopy (Carabajal and Harding, 2006).

6.4. Elevation Comparison

To evaluate which DEM better represents the actual terrain it is necessary to make a comparison with independent reference data. The reference data in this study are the 57 GCPs shown in Figure 2. These GCPs do not cover the whole study area, but only an area of 1750 m × 2250 m. Elevations were extracted from ASTER2 and SRTM, corresponding to the GCPs. Statistical analyses were performed to investigate the GCPs and the corresponding points from STRM and ASTER2, and to estimate the vertical accuracy of the two elevation models. Spearman correlation test (two-tailed) was conducted between the three point datasets (GCPs and corresponding points from SRTM and ASTER2) to assess the goodness of SRTM and ASTER2. There was a positive correlation between SRTM and GCPs (correlation coefficient, $r = 0.5$; sample size, $n = 57$; significance level, $p < 0.05$) but there was no significant correlation in the case of ASTER2 ($r = 0.29$, $n = 57$, $p > 0.05$). Table 2 shows the results of correlation analysis between GCPs and the corresponding points of the other two DEMs. Figure 8 shows the histograms for elevation difference between the reference data and the corresponding points from the other two DEMs. As can be seen, the SRTM error follows a Gaussian normal distribution. ASTER2 error, on the other hand, does not show a normal distribution. In both cases, SRTM and ASTER2 error histograms have their peaks at around 4 m, with no negative values in both cases, which means that in all cases the DEMs overestimate the reference elevations and the elevation difference is less in the case of SRTM.

A practicable method for comparing the elevation accuracy is the RMSE, which is a common measure for quantifying the vertical accuracy of DEMs. The RMSE for ASTER2

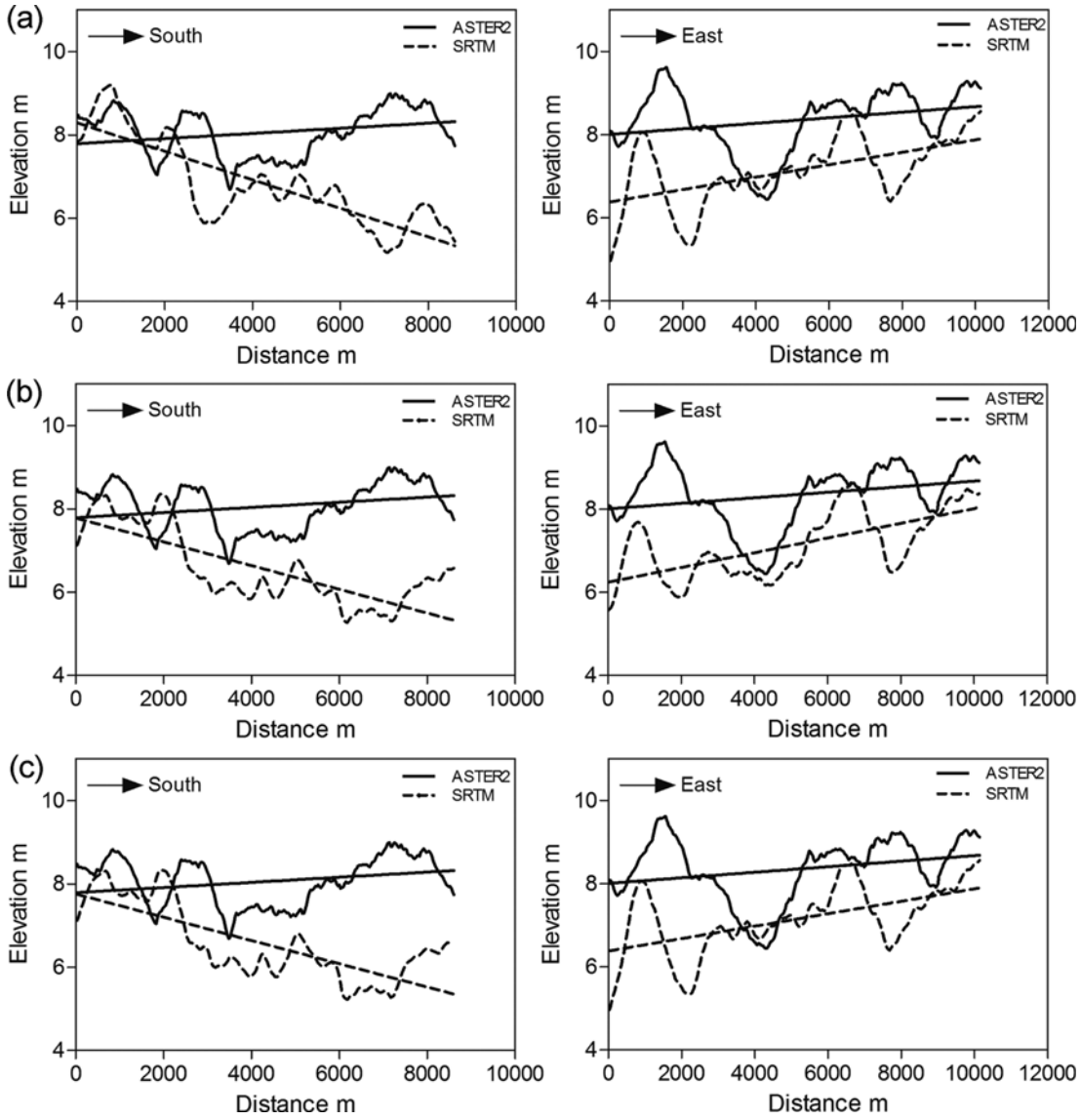

Fig. 7. Latitudinal (left) and longitudinal (right) topographic profiles (using 10-period moving average) through DEMs in Titas Upazila, after resampling SRTM to ASTER2 resolution using three methods, (a) Nearest Neighbor (b) Bilinear and (c) Cubic. Dashed and continuous straight lines represent the trend lines through the profiles of SRTM and ASTER2 models, respectively.

Table 2. Results of Spearman correlation test (two-tailed) between the 57 GCPs and the corresponding points from the two elevation models SRTM and ASTER2

	r (correlation coefficient)	P-value (significance level)
ASTER2	0.29	>0.05
SRTM	0.5	<0.05

and SRTM was calculated in relation to the reference data, and the statistical results are summarized in Table 3. It can be inferred from Table 3 that SRTM has slightly smaller minimum, mean, and RMSE values than ASTER2. The SD is identical for SRTM, ASTER2, and the reference data, which means that elevation values have similar ranges. The mean values of GCPs and corresponding points from both DEMs are partly biased. Moreover, there is a difference between the RMSE (5) of ASTER2 calculated in relation to the reference data (GCPs) and RMSE (7.53) calculated using Equation (1). This difference can be attributed to either Equation (1) offering only a rough estimation of RMSE or to this equation being estimated using ASTER GDEM v1, the result of which does not hold for the ASTER GDEM v2 (ASTER2) used in this study.

7. SRTM DEM MODIFICATION

This section outlines a method for the quality improvement of SRTM data to produce more detailed high-resolution DTM for improved hydrological modeling. The improvement is

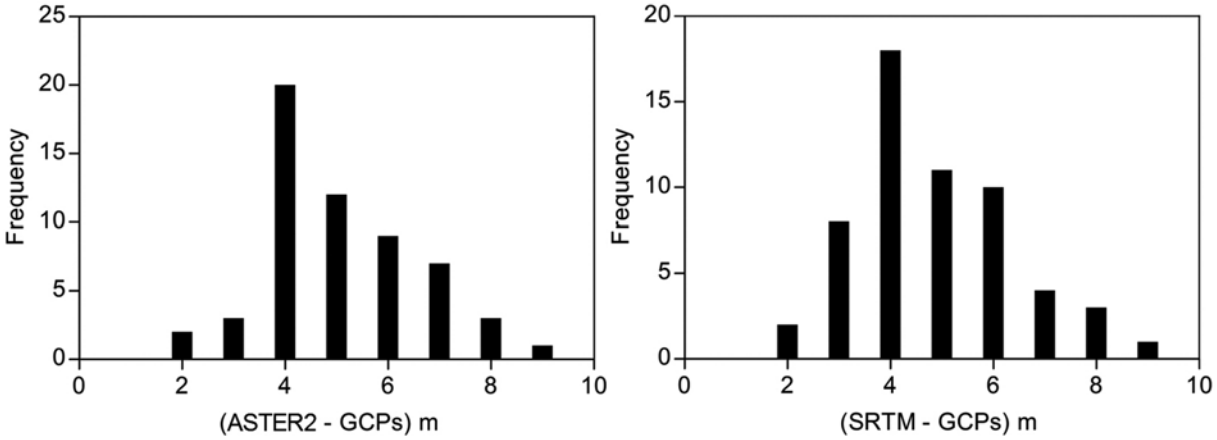

Fig. 8. Error histograms comparing GCPs elevation and the corresponding SRTM and ASTER2 pixels.

Table 3. Statistic results of inter-comparisons of the DEMs with the 57 GCPs over the study area in Bangladesh

	Mean (m)	Min (m)	Max (m)	SD (m)	Kurtosis[a]	Skewness[a]	root mean square error RMSE (m)
ASTER2	8	6	11	1.4	–0.7	–0.2	5
SRTM	7.7	5	11	1.2	–0.2	0.1	4.5
57 GCPs	3.3	1.9	5.7	1.3	–0.5	1	

[a]Unitless number.

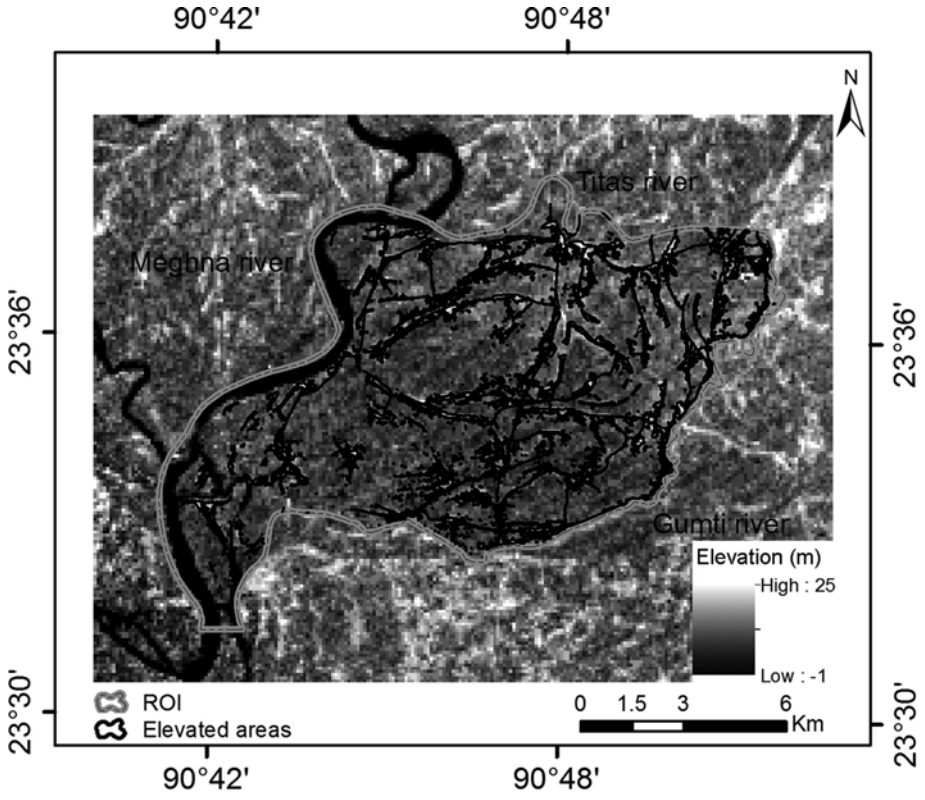

Fig. 9. SRTM DEM raster draped by the digitized elevated areas.

focused on representing the manmade topographic features (e.g., road embankments and mounds that houses are built on above the monsoon flooding level), which are not represented or not completely represented in the DEM. The focus here will be on the part of the whole area mentioned before that is located within the ROI polygon, as shown in Figure 9. It is bordered by three rivers (Meghna, Gumti, and Titas). The study area is flat terrain with artificially elevated areas where

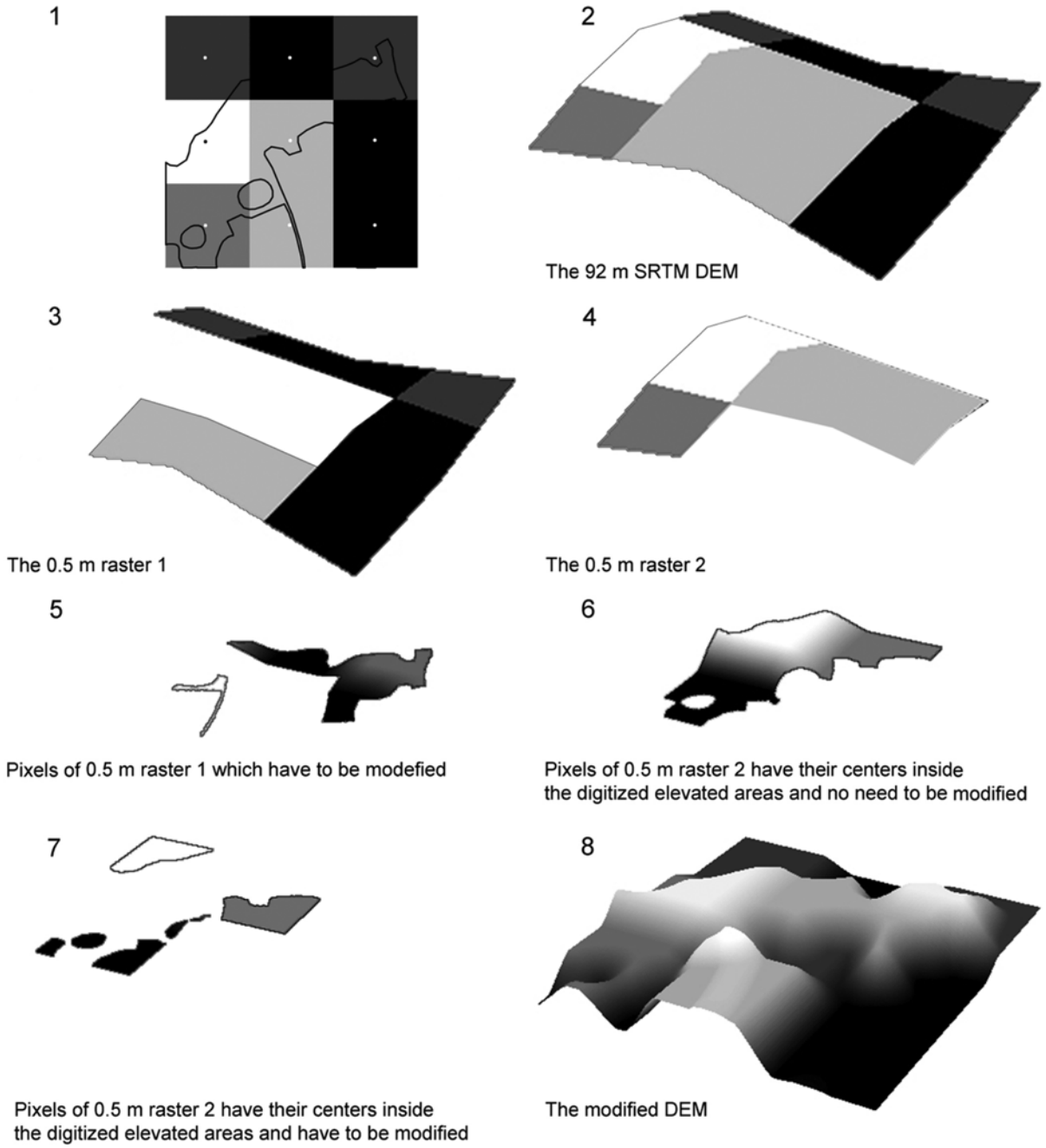

Fig. 10. Modification steps of SRTM.

people live. Normally, these elevated residential areas are not represented in SRTM data except in some parts where the center of the pixel is located on the elevated areas.

To represent the elevated areas in the SRTM, this model was modified by giving the elevated areas their real elevations. The extent of these areas varies from place to place and the average elevation difference against the neighborhood is 3 m (Planer-Friedrich et al., 2012). Elevated areas were digitized in ArcGIS Desktop 9.3 using GeoEye satellite image. Because the GeoEye image did not cover the whole study area, Google Earth was used to delineate the rest of the region of interest. The digitized elevated areas are shown in Figure 9. Figure 10 shows the steps followed to modify the SRTM DEM, which are as follows:

(1) Step 1 (Fig. 10) shows a 2D representation of a small area of the DEM draped by the digitized polygon; step 2 shows a 3D representation of the same area.

(2) Pixels that already had a true elevation were separated from the rest of the elevation model. This was done by converting the whole DEM to a point shapefile, then the points

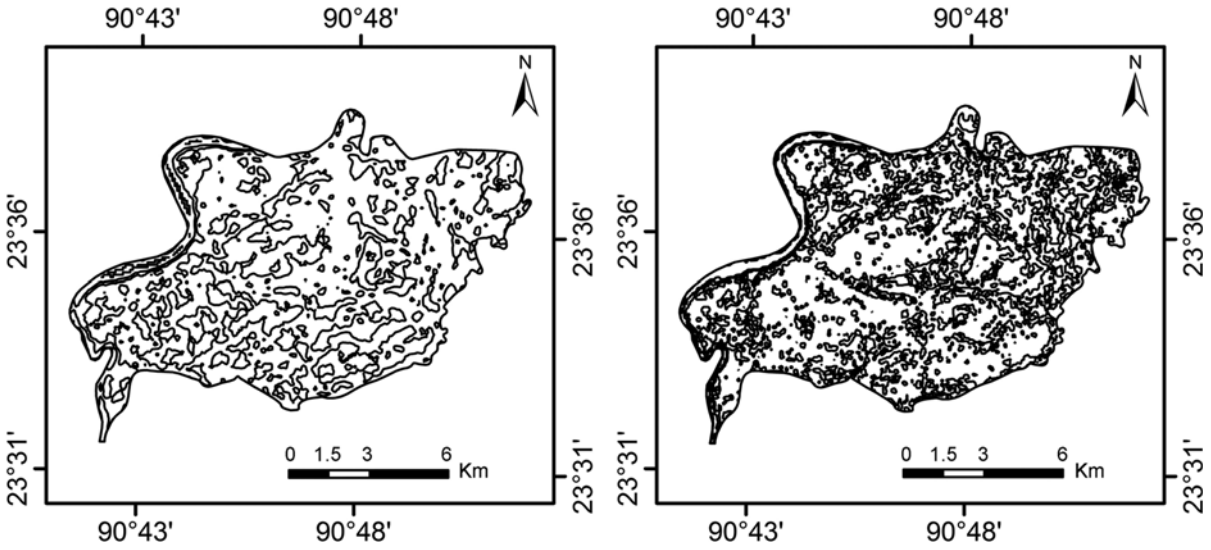

Fig. 11. Contour maps (3 m interval) of the area of interest before (left) and after (right) modification regarding the residence elevated areas.

located within the digitized polygons were extracted and converted to raster 2 and the rest of the points converted to raster 1. Both rasters 1 and 2 were resampled to 0.5 m (steps 3 and 4 in Fig. 10).

(3) Pixels from the 0.5 m resampled raster 1 corresponding to the manmade elevated areas were identified and modified by the polygons digitized previously. These pixels were extracted from raster 1 and given a real elevation using the raster calculator (step 5 in Fig. 10).

(4) Due to the original big pixel size of raster 2 (92 m) and the small extent of the manmade elevated areas (2 m in some parts), the 0.5 m resampled raster 2 had some 0.5 m pixels with true elevation values inside the digitized polygons and other pixels outside the digitized polygons, which had to be modified. Pixels inside the digitized polygons were kept without modification (step 6 in Fig. 10).

(5) Erroneous 0.5 m pixels from the resampled raster 2 located outside the digitized polygons were modified (their elevation is overestimated). Modification of these pixels was done by extracting them from the resampled raster 2 and subtracting the average elevation of the elevated areas from their original elevation (step 7 in Fig. 10).

(6) Finally, all the modified pixels were mosaicked with the original DEM resampled to 0.5 m (step 8 in Fig. 10).

Moreover, there is a positive bias (ca. 4.4 m) between GCPs and corresponding pixels from the SRTM. A simple method was applied to eliminate this bias in two steps. First, the mean (value) of the differences between the GCPs and the corresponding points of the SRTM model was subtracted from SRTM points, which diminished the RMSE to 0.67 m. Second, the same averaged difference was subtracted from the whole SRTM model. The topographic maps of the elevation model before (left) and after (right) these modifications are shown in Figure 11. The contour lines based on the modified SRTM DEM in relation to the original SRTM DEM show the strong influence of the modification on the morphologic details of the DEM. The elongated artificially elevated residential areas are clearly more pronounced in the modified DEM in comparison to the original elevation model.

8. CONCLUSIONS

This study compared the quality of two DEMs (SRTM C-band CGIAR-CSI v4.1 and ASTER GDEM v2) for a study area in Bangladesh. The two elevation models were compared from different aspects, and their accuracy was estimated by means of GCPs. Although ASTER GDEM v2 30 m has a higher resolution than SRTM C-band CGIAR-CSI v4.1 and is expected to be nine times more detailed than SRTM C-band CGIAR-CSI v4.1, it can be concluded from the previous discussion and our own investigations that ASTER GDEM v2 has many more pitfalls than SRTM C-band CGIAR-CSI v4.1, at least in flat terrain. These pitfalls can be summarized as follows:

· Spatial shift exists in both elevation models, which could be calculated using the very high resolution (VHR) GeoEye satellite image. For SRTM C-band CGIAR-CSI v4.1, 53 m in x direction and 11 m in y direction were calculated, while 26 m in x direction and 24 m in y direction were calculated for ASTER GDEM v2. The shift is clearly less in the SRTM C-band CGIAR-CSI v4.1 than in ASTER GDEM v2 with respect to the pixel size.

· SRTM C-band CGIAR-CSI v4.1 is more detailed from a morphological point of view than the ASTER GDEM v2. Streams and river channels are not presented in the higher resolution ASTER GDEM v2 elevation model in the study area. Existing water bodies are represented in some parts of ASTER GDEM v2 as elevated areas and reach up to 30 m in

some parts of the study area. Poor elevation data in ASTER GDEM v2 is related to low stack number and to not flattening the water surface using a water mask, as in case of SRTM C-band CGIAR-CSI v4.1.

· Slope is also an important parameter in hydrological and hydrogeological applications. The tested models showed different slopes in different directions. This was checked by comparing the cross sections through the datasets. The most pronounced difference was in the north-south direction. Here, the SRTM C-band CGIAR-CSI v4.1 also better mimics the reality by showing an incline towards the outlet of the basin.

· The elevation models investigated in this study overestimate the true terrain in all parts without exception. The correlation test between the two DEMs and the GCPs revealed that SRTM C-band CGIAR-CSI v4.1 has a positive correlation of $r = 0.5$ that was significant at the 0.05 level (two-tailed), and it represents better the real topographic surface. On the other hand, the correlation was not significant at the same confidence level in the case of ASTER GDEM v2 ($r = 0.29$, $p > 0.05$). The difference in the RMSE for ASTER GDEM v2 (5 m) and SRTM C-band CGIAR-CSI v4.1 (4.5 m) in relation to the GCPs is not so significant; nevertheless, this difference (0.5) in RMSE in flat terrain (as in the study area) might be significant for some applications.

· It is known, due to the wavelength difference, that radar-based measurements used by SRTM C-band are less affected by atmospheric conditions than the regular optical wavelength-based systems such as ASTER (Forkuor and Maathuis 2012). The longer the wavelength, the better the satellite system may peer through cloud cover. This characteristic makes the use of SRTM C-band CGIAR-CSI v4.1 preferable to ASTER GDEM v2 in tropical areas, where a dense cloud cover is very likely.

· In accordance with the conclusions above, the SRTM C-band CGIAR-CSI v4.1 elevation model was selected to represent the terrain in the study area. One problem in this elevation model, which is related to the insufficient spatial resolution, is the manmade residential elevated areas, which have an elevation difference of almost 3 m from the surrounding areas and vary in extent all over the study area. Digitizing these residential areas and roads and resampling the original DEM, then changing the elevation of some pixels within these areas, enabled us to represent these missing features. Even though the presented approach for editing the DEM is highly manual and this method is not applicable everywhere, it can be used in some areas of the world where no accurate and detailed models are available, such as in Bangladesh. It is worth mentioning that the improved elevation model needs validation, which is not done in this research paper due to the small number of available GCPs (57 points) that are not distributed over the entire study area. Validation could be achieved by identifying some points on the elevation model and on the ground, then measuring the real elevations above sea level and comparing them with the corresponding elevations from the improved model.

· A two-step methodology is applied to eliminate the positive bias (4.4 m) between the GCPs and the SRTM. The first step is finding the mean (value) of the differences between the GCPs and the corresponding points of the SRTM model, and the second step is subtracting the calculated mean from the whole SRTM C-band CGIAR-CSI v4.1 model.

ACKNOWLEDGMENTS: This work was funded by the Syrian Ministry of Higher Education. The authors are grateful to the GeoEye Foundation Employee Advisory Committee (FEAC) for the imagery grant. The freely available ASTER GDEM v2 is the property of METI and NASA and to be downloaded from EROS DAC and NASA's LPDAAC. SRTM Version 4 for the globe is available at no charge from CGIAR-CSI SRTM Database. We thank two anonymous reviewers for their comments by which the manuscript could be improved significantly.

REFERENCES

Ahmad, B.B., 2009, Assessment and correction of SRTM DEM with reference to Geo-hazard identification in the Cameron highlands, Malysia. Geoinformation Science Journal, 9, 32–40.

Arefi, H. and Reinartz, P., 2011, Accuracy enhancement of ASTER global digital elevation models using ICESat data. Remote Sensing, 3, 1323–1343.

ASPRS Map Accuracy Working Group., 2014, ASPRS Positional Accuracy Standards for Digital Geospatial Data REVISION 7, VERSION 1, FINAL DRAFT FOR BOARD APPROVAL, 53 p.

ASTER GDEM Validation Team, 2009, ASTER Global DEM Validation Summary Report. Prepared by: METI, NASA, USGS in cooperation with NGA and Other Collaborators, 28 p.

Bekithemba, G., Nelson, M., George, S., and Hubert, H.G.S., 2002, Coupling of Digital Elevation Model and Rainfall-Runoff Model in Storm Drainage Network Design. Physics and Chemistry of the Earth, Parts A/B/C, 27, 755–764.

Braun, A. and Fotopoulos, G., 2007, Assessment of SRTM, ICESat, and Survey Control Monument Elevations in Canada. Photogrammetric Engineering & Remote Sensing, 73, 1333–42.

Carabajal, C. and Harding, D., 2006, SRTM C-Band and ICESat Laser Altimetry Elevation Comparisons as a Function of Tree Cover and Relief. Photogrammetric Engineering & Remote Sensing, 72, 287–298.

Casana, J. and Cothren, J., 2008, Stereo analysis, DEM extraction and orthorectification of CORONA satellite imagery: archaeological applications from the Near East. Antiquity, 82, 732–749.

Chorowicz, J., Scanvic, J.Y., Rouzeau, O., and Cuervo, G.V., 1998, Observation of recent and active landslides from SAR ERS-1 and JERS-1 imagery using a stereo-simulation approach: Example of the Chicamocha valley in Colombia. International Journal of Remote Sensing, 19, 3187–3196.

Congalton, R.G. and Green, K., 2008, Assessing the Accuracy of Remotely Sensed Data: Principles and Practices (2nd Edition). CRC Press, London, 200 p.

Creed, I. and Sass, G., 2011, Digital Terrain Analysis Approaches for Tracking Hydrological and Biogeochemical Pathways and Processes in Forested Landscapes. In: Levia, D.F., Carlyle-Moses, D., and Tanaka, T. (eds), Forest Hydrology and Biogeochemistry SE – 4. Ecological Studies. Springer Netherlands, 216, 69–100.

Forkuor, G. and Maathuis, B., 2012, Comparison of SRTM and ASTER Derived Digital Elevation Models over Two Regions in

Ghana – Implications for Hydrol Ogical and Environmental Modeling. In Studies on Environmental and Applied Geomorphology, edited by Tommaso Piacentini and Enrico Miccadei. InTech, 23 p. http://www.intechopen.com/books/studies-on-environmental-and-applied-geomorphology/comparison-of-srtm-and-aster-derived-digital-elevation-models-over-two-regions-in-ghana.

Frey, H. and Paul, F., 2012, On the suitability of the SRTM DEM and ASTER GDEM for the compilation of topographic parameters in glacier inventories. International Journal of Applied Earth Observation and Geoinformation, 18, 480–490.

Gonçalves, J.A. and Morgado, A.M., 2008, Use of the SRTM DEM as a Geo-Referencing Tool by Elevation Matching. The International Archives of the Photogrammetry, Remote Sensing and Spatial Information Sciences, XXXVII, 879–884.

Guo-an, T., Strobl, J., Jian-ya, G., Mu-dan, Z., and Zhen-jiang, C., 2001, Evaluation on the Accuracy of Digital Elevation Models. Journal of Geographical Sciences, 11, 209–216.

Guth, P., 2010, Geomorphometric comparison of ASTER DEM and SRTM. Proceedings of a Special Joint Symposium of ISPRS Technical Commission IV & AutoCarto, Orlando, Nov. 15–19, p. 10.

Harvey, C.F., Ashfaque, K.N., Yu, W., Badruzzaman, A.B.M., Ali, M.A., Oates, P.M., Michael, H.A., Neumann, R.B., Beckie, R., Islam, S., and Ahmed, M.F., 2006, Groundwater dynamics and arsenic contamination in Bangladesh. Chemical Geology, 228, 112–136.

Hirano, A., Welch, R., and Lang, H., 2003, Mapping from ASTER stereo image data: DEM validation and accuracy assessment. ISPRS Journal of Photogrammetry and Remote Sensing, 57, 356–370.

Hirt, C., Filmer, M.S., and Featherstone, W.E., 2010, Comparison and validation of the recent freely-available ASTER-GDEM ver. 1, SRTM ver. 4.1 and GEODATA DEM – 9S ver. 3 digital elevation models over Australia. Australian Journal of Earth Sciences, 57, 337–347.

Isioye, O.A. and Jobin, P., 2012, An assessment of digital elevation models (DEMs) from different spatial data sources. Asian Journal of Engineering, Sciences & Technology, 2, 1–17.

Jacobsen, K., 2005, DEMs Based on Space Images versus SRTM Height Models. Proceedings of ASPRS Annual Conference on Geospatial Goes Global: From Your Neighborhood to the Whole Planet, Baltimore, March 7–11, p. 9.

Jacobsen, K. and Passini, R., 2010, Analysis of ASTER GDEM Elevation Models. The International Archives of the Photogrammetry, Remote Sensing and Spatial Information Sciences, XXXVIII, p.6.

Jacobsen, K., 2003, DEM generation from satellite data. Proceedings of EARSel Symposium on Remote Sensing in Transition, Ghent, June 2–5, p. 513–525.

Jarvis, A., Rubiano, J., Nelson, A., Farrow, A., and Mulligan, M., 2004, Practical use of SRTM data in the tropics – Comparisons with digital elevation models generated from cartographic data. Working document no. 198, International Center for Tropical Agricultura, Cali, Colombia, 38 p.

Kanoua, W. and Merkel, B., 2015, Groundwater recharge in Titas Upazila in Bangladesh. Arabian Journal of Geosciences, 8, 1361–1371.

Kavanagh, B.F. and Bird, S.J.G., 2000, Surveying: Principles and Applications (5th Edition). Prentice Hall, Upper Saddle River, 722 p.

Khan, M.K.A., Alam, M., Islam, M.S., Hassan, M.Q., and Al-Mansur, M.A., 2011, Environmental Pollution Around Dhaka EPZ and its Impact on Surface and Groundwater. Bangladesh Journal of Scientific and Industrial Research, 46, 153–162.

Mikhail, E.M., Bethel, J.S., and McGlone, J.C., 2001, Introduction to Modern Photogrammetry. Wiley, New York, 479 p.

Konstantinos, N. and Antonis, A., 2004, Creation of DTM with ASTER Data and Statistical Verification of the Accuracy of the Model (Western Peloponnese, Greece). Geocarto International, 19, 3–9.

Lane, S.N., Richards, K.S., and Chandler, J.H., 1994, Developments in monitoring and modelling small-scale river bed topography. Earth Surface Processes and Landforms, 19, 349–368.

Luijendijk, E., Person, M., Balen, R.V., Voorde, M.T., Verweij, H., and Simmelink, E., 2010, The effect of topography driven groundwater flow on deep subsurface temperatures in the Roer Valley Graben (southern Netherlands). Proceedings of American Geophysical Union Fall Meeting (Abstract# V13B-2361), San Francisco, Dec. 13–17, p. 2361.

Martinoni, D. and Bernhard, L., 1998, A conceptual framework for reliable digital terrain modelling. Proceedings of the 8th Symposium on Spatial Data Handling. Vancouver, p. 737–750.

Menze, B.H., Ur, J.A., and Sherrat, A.G., 2006, Detection of Ancient Settlement Mounds: Archaeological Survey Based on the SRTM Terrain Model. Photogrammetric Engineering & Remote Sensing, 72, 321–327.

Moore, I.D., Grayson, R.B., and Ladson, A.R., 1991, Digital terrain modelling: A review of hydrological, geomorphological, and biological applications. Hydrological Processes, 5, 3–30.

Nikolakopoulos, K.G., Kamaratakis, E.K., and Chrysoulakis, N., 2006, SRTM vs. ASTER elevation products. Comparison for two regions in Crete, Greece. International Journal of Remote Sensing, 27, 4819–4838.

Pilesjö, P. and Hasan, A., 2014, A Triangular Form-based Multiple Flow Algorithm to Estimate Overland Flow Distribution and Accumulation on a Digital Elevation Model. Transactions in GIS, 18, 108–124.

Planer-Friedrich, B., Härtig, C., Lissner, H., Steinborn, J., Süß, E., Qumrul, H.M., Zahid, A., Alam, M., and Merkel, B., 2012, Organic carbon mobilization in a Bangladesh aquifer explained by seasonal monsoon-driven storativity changes. Applied Geochemistry, 27, 2324–2334.

Podobnikar, T., Stancic, Z., and Oštir, K., 2000, Data integration for the DTM production. Proceedings of International Society for Photogrammetry and Remote Sensing WG VI/3 and IV/3 meeting: Bridging the Gap, Ljubljana, Feb. 2–5, p. 7.

Reuter, H.I., Nelson, A., Strobl, P., Mehl, W., and Jarvis, A., 2009, A First Assessment of ASTER GDEM Tiles for Absolute Accuracy, Relative Accuracy and Terrain Parameters. Proceedings of IEEE International Geoscience and Remote Sensing Symposium, Cape Town, July 12–17, p. 240–243.

Rexer, M. and Hirt, C., 2014, Comparison of Free High Resolution Digital Elevation Data Sets (ASTER GDEM2, SRTM v2.1/v4.1) and Validation against Accurate Heights from the Australian National Gravity Database. Australian Journal of Earth Sciences, 61, 213–26.

Rodriguez, E., Morris, C.S., and Belz, E.J., 2006, A Global Assessment of the SRTM Performance. Photogrammetric Engineering and Remote Sensing, 72, 249–260.

Saldana, M.M., Aguilar, M.A., Aguilar, F.J., and Fernandez, I., 2012, DSM extraction and evaluation from GeoEye-1 stereo imagery. ISPRS Annals of the Photogrammetry, Remote Sensing and Spatial Information Sciences, I-4, 113–118.

Sefercik, U. and Alkan, M., 2009, Advanced analysis of differences between C and X bands using SRTM data for mountainous

topography. Journal of the Indian Society of Remote Sensing, 37, 335–349.

Sertel, E., 2010, Accuracy assessment of ASTER global DEM over Turkey. Proceedings of a special joint symposium of ISPRS Technical Commission IV & AutoCarto, Orlando, Nov. 15–19, p. 5.

Simard, M., Zhang, K., Rivera-Monroy, V.H., Ross, M.S., Ruiz, P.L., Castañeda-Moya, E., Twilley, R.R., and Rodriguez, E., 2006, Mapping Height and Biomass of Mangrove Forests in Everglades National Park with SRTM Elevation Data. Photogrammetric Engineering & Remote Sensing, 72, 299–311.

Singhroy, V., Mattar, K.E., and Gray, A.L., 1998, Landslide characterisation in Canada using interferometric {SAR} and combined {SAR} and {TM} images. Advances in Space Research, 21, 465–476.

Small, D., 1998, Generation of Digital Elevation Models through Spaceborne SAR Interferometry. Ph.D. thesis, University of Zürich, Zürich, 168 p.

Smith, B. and Sandwell, D., 2003, Accuracy and resolution of shuttle radar topography mission data. Geophysical Research Letter, 30, 1–4.

Stevens, N.F., Garbeil, H., and Mouginis-Mark, P.J., 2004, NASA EOS Terra ASTER: Volcanic topographic mapping and capability. Remote Sensing of Environment, 90, 405–414.

Sunahara, T., Nmor, J.C., Goto, K., Futami, K., Sonye, G., Akweywa, P., Dida, G., and Minakawa, N., 2003, Topographic models for predicting malaria vector breeding habitats: potential tools for vector control managers. Parasites & Vectors, 6, 1–13.

Tachikawa, T., Kaku, M., Iwasaki, A., Gesch, D., Oimoen, M., Zhang, Z., Danielson, J., Krieger, T., Curtis, B., Haase, J., Abrams, M., Crippen, R., and Carabajal, C., 2011, ASTER Global Digital Elevation Model Version 2 – Summary of Validation Results. Archive Center and the Joint Japan-US ASTER Science Team, 27 p.

Turton, D. and Jonas, D., 2003, Airborne Laser Scanning - Cost Effective Spatial Data. Proceedings of Map Asia 2003 Conference, Kuala Lumpur, Oct. 13–15, AD1.

Urai, M., Tachikawa, T., and Fujisada, H., 2012, Data Acquisition Strategies for ASTER GLOBAL DEM Generation. ISPRS Annals of Photogrammetry, Remote Sensing and Spatial Information Sciences, I-4, 199–202.

Yastikli, N., Koçak, G., and Büyüksalih, G., 2006, Accuracy and Morphological Analyses of GTOPO30 and SRTM X-C Band DEMs in the Test Area Istanbul. Proceedings of ISPRS Topographic Mapping from Space Workshop, Ankara, Feb. 14–16, p. 6.

Manuscript received July 17, 2014
Manuscript accepted April 14, 2015